A&A 402, L35–L38 (2003)
DOI: 10.1051/0004-6361:20030336

Astronomy & Astrophysics

The Odin satellite⋆

II. Radiometer data processing and calibration

M. Olberg[1], U. Frisk[2], A. Lecacheux[3], A. O. H. Olofsson[1], P. Baron[3], P. Bergman[1], G. Florin[2], Å. Hjalmarson[1], B. Larsson[4], D. Murtagh[5], G. Olofsson[4], L. Pagani[6], Aa. Sandqvist[4], D. Teyssier[7], S. A. Torchinsky[8], and K. Volk[9]

[1] Onsala Space Observatory, 439 92 Onsala, Sweden
[2] Swedish Space Corporation, PO Box 4207, 171 04 Solna, Sweden
[3] LESIA, Observatoire de Paris, Section de Meudon, 5 place Jules Janssen, 92195 Meudon Cedex, France
[4] Stockholm Observatory, SCFAB, Roslagstullsbacken 21, 106 91 Stockholm, Sweden
[5] Global Environmental Measurements Group, Chalmers University of Technology, 412 96 Göteborg, Sweden
[6] LERMA & FRE 2460 du CNRS, Observatoire de Paris, 61 Av. de l'Observatoire, 75140 Paris, France
[7] SRON, Postbus 800, 9700 AV Groningen, The Netherlands
[8] Canadian Space Agency, St-Hubert, J3Y 8Y9, Québec, Canada
[9] Department of Physics and Astronomy, University of Calgary, Calgary, ABT 2N 1N4, Canada

Received 2 December 2002 / Accepted 25 January 2003

Abstract. The radiometer on-board the Odin satellite comprises four different sub-mm receivers covering the 486–581 GHz frequency range and one fixed frequency 119 GHz receiver. Two auto-correlators and one acousto-optical spectrometer serve as backends. This article gives an overview over the processing of the data delivered by these instruments and discusses calibration issues.

Key words. space vehicles: instruments – submillimeter – techniques: spectroscopic – telescopes

1. Introduction

The calibration of radio observations from satellites differs in a number of aspects from that of ground-based observations. On the one hand the main difficulty for radio telescopes on ground, namely to properly account for the attenuation of the signal by the Earth's atmosphere, is no longer an issue. On the other hand the much more indirect operation of a satellite borne telescope has challenges of its own. The thermal and electrical environment of a satellite may cause receiver instabilities, which must be compensated. Whereas ground based systems may have relatively stable gain but changing system temperature due to unstable weather conditions, the Odin satellite shows the opposite behaviour: stable noise figures in spite of cyclic gain variations during one orbit.

Typically, an observing program is uploaded during passages above the ground station and the processing needs to make sure that the downloaded telemetry data is compatible with the intended observation. Also, satellites normally lack the means to compensate in real-time for Doppler effects introduced by the orbital motion of the satellite around the Earth ($v_{\rm sat} \approx 7\,{\rm km\,s^{-1}}$). As a consequence short time integrations are performed, which are subsequently aligned on a rest frequency scale by the processing software. This leads to high data volumes with an immediate need for some kind of processing pipeline. Failing instruments cannot be repaired, and instead the processing needs to be adapted to new situations.

Odin is a sub-mm satellite with a dual mission: astronomy and aeronomy. Odin observing time is split evenly between these two disciplines: the search for mainly water and oxygen emission from astronomical objects (Hjalmarson et al. 2003) and observations of the Earth's atmosphere in order to map, the distribution of molecules relevant in the context of ozone depletion (Murtagh et al. 2002).

2. Basic technical specification

The satellite orbits the Earth in a sun-synchronous orbit at an altitude of ≈600 km, passing the ground station at Esrange in northern Sweden about fourteen times a day. The 1.1 m offset Gregorian telescope has a beam width of 2′ and 9′ at 500 GHz and 119 GHz, respectively. From Jupiter observations we

Send offprint requests to: M. Olberg,
e-mail: olberg@oso.chalmers.se

⋆ Odin is a Swedish-led satellite project funded jointly by the Swedish National Space Board (SNSB), the Canadian Space Agency (CSA), the National Technology Agency of Finland (Tekes) and the Centre National d'Études Spatiales (CNES, France). Odin is operated by the Swedish Space Corporation (SSC), the project's prime industrial contractor.

Table 1. Odin frontend and backend frequency specifications. AC1 and AC2 denote the two correlators, for which the four main configurations are listed.

frontend	tuning range GHz	backend	bandwidth MHz	channel spacing MHz
549 A1	541–558	AOS	1050	0.61
495 A2	486–504	AC1/AC2	800	1.0
555 B1	547–564		400	0.5
572 B2	563–581		200	0.25
119 C	118.75		100	0.125

estimate a main beam efficiency of $\eta_{\rm mb} \approx 0.9$. Pointing accuracy is better than 10″.

The satellite is equipped with four sub-mm receivers. Table 1 lists their single sideband (SSB) tuning ranges. In addition a fixed frequency millimeter receiver covering the ground transition of molecular oxygen operates near 119 GHz. Typical single-sideband system temperatures are 3300 K and 600 K for the sub-mm and mm receivers, respectively.

The receivers form two groups, A1+A2 and B1+B2+C, where each group shares a common path through the beam optics. Consequently, in Dicke switching mode one group will receive its signal via the main beam when the other sees the reference signal, and vice versa. This design also implies, that in position switched mode only one group can be used at the same time.

Three spectrometers, one acousto-optical spectrometer and two auto-correlators of hybrid type can be connected to the receivers in a number of ways. In addition, signal combiners allow one correlator to be shared between two sub-mm receivers.

A 3-channel filter bank, slaved to one of the correlators, is used in aeronomy mode to monitor emission in the 119 GHz band in order to derive estimates of atmospheric temperature and pressure.

A block diagram showing the arrangements of receivers and spectrometers is presented in Frisk et al. (2003), who describe other technical aspects of the radiometer. The same diagram also outlines the main features of the beam optics.

3. Observing modes

The main observing mode is by switching against the cold sky, by means of a chopper-wheel, between the main beam and an unfocused sky beam of 4.4° FWHM at all wavelengths. Integration times per phase are between 1 and 10 s. An internal selection mirror can choose between two possible directions of the sky beam, separated by 28°. The separation from the main beam amounts to 42°. In astronomy mode the sky beam is chosen such that contamination from solar system objects and the Galactic plane is avoided. In aeronomy, the beam pointing away from the Earth is used.

For calibration purposes the selection mirror may also direct the beam towards an internal load at ambient temperature.

Due to a sun constraint Odin's main beam is always within 30° of the orbital plane, and for about one third of the orbit the astronomical object will be occulted by the Earth

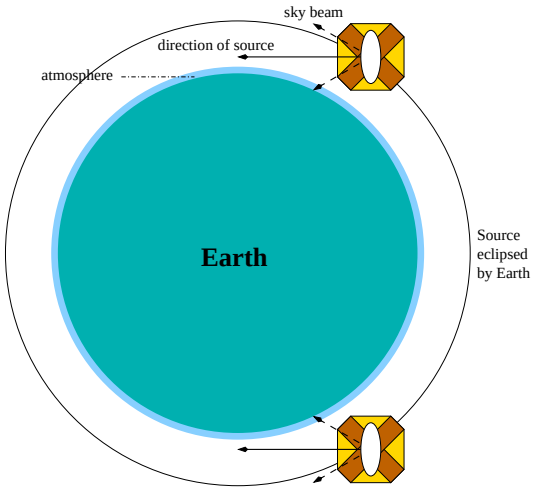

Fig. 1. The astronomy orbit. Two thirds of the orbit are available for target observation, the remaining part is occulted by the Earth. During one orbit the Earth's atmosphere is scanned twice. The main beam points in the direction of the source. The two sky beam directions are indicated by dashed lines.

(see Fig. 1). This leaves about two thirds of the time, or roughly 60 min per orbit, for target observations. During this time the Doppler shift due to the satellite's motion will change from -7 km s^{-1} to $+7$ km s^{-1}, which subsequently needs to be corrected for as part of the on-ground data processing.

On entering and leaving the occulted part the telescope beam will pick up a signal from the terrestrial atmosphere, which can be used for accurate frequency calibration.

Figure 2 shows the mean intensity across all channels of one of the spectrometers during the course of one astronomy orbit of Dicke switched observations. Data from different beam directions (main beam, sky beam and internal load) are labelled. The typical gain variation due to a changing thermal environment during one orbit is clearly seen. Main beam data are at a higher level compared to cold sky due to thermal emission from a baffle.

It turns out that the slight imbalance between signal and reference phase introduces instabilities seen as low-level ripple in the spectrometer passbands. This ripple is stable in the IF band, and can be measured towards a blank region of the sky and subsequently be subtracted from target spectra. A figure showing the noise level at 119 GHz as function of time is available in Pagani et al. (2003).

In position switched observations the satellite is moved between target and off position about once per minute, while data readout still occurs every few seconds, to prevent deterioration of the frequency resolution due to Doppler effects. While this avoids the above mentioned ripple, the system is more sensitive to gain variations as switching is not as fast in this mode.

4. Calibration scheme

The calibration scheme is based on the assumption that the digital value c_i read out from channel i of a spectrometer and normalised by division by integration time, is proportional to the

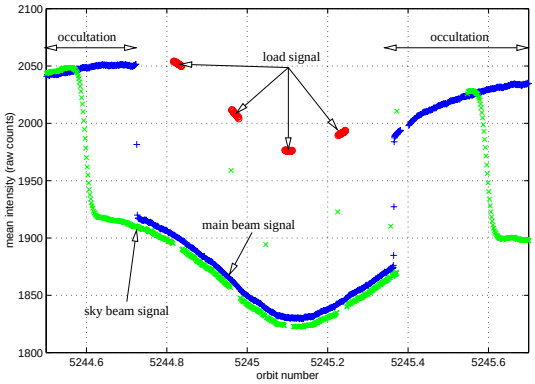

Fig. 2. Intensity variations during an astronomy orbit. The mean intensity over all channels from one spectrometer is shown. Data observed by the different beams are labelled. The occulted phase is clearly seen as high intensity values for the main beam. Switching is performed against the sky beam which is furthest away from the Earth. Some intermediate intensity values are due to the fact, that the spectrometers outputs are not blanked during movements of the selection mirror.

observed signal. The contributions to the signal are expressed as equivalent Rayleigh-Jeans temperatures:

$$c_i^b = g_i \left(\eta^b T_{b,i} + (1-\eta^b) T_{\mathrm{amb},i} + T_{\mathrm{sys},i}\right). \quad (1)$$

This is applied to all three different beam selections b, namely antenna main beam (A), sky beam (S) and internal load (L). The integrated gain over each beam is η^b, and expresses the fact that part of the beam is terminated at ambient temperature T_{amb}. The term $T_{\mathrm{sys},i}$ represents common system noise, which for a satellite borne system is equal to the receiver noise. For the cold sky and internal load we can take the black-body radiation as being independent of frequency (over the ≤1.1 GHz bandwidth of an Odin spectrometer): $T_{\mathrm{L},i} = T_{\mathrm{L}}$ and $T_{\mathrm{S},i} = T_{\mathrm{S}}$ for all i. For the internal load the term T_b is replaced by ϵT_{L} to allow for a non-perfect emissivity of the load material. Combining Eq. (1) for the sky and load beam, the gain g_i for channel i is calculated as

$$g_i = \frac{c_i^{\mathrm{L}} - c_i^{\mathrm{S}}}{\eta^{\mathrm{L}}\epsilon T_{\mathrm{L}} - \eta^{\mathrm{S}} T_{\mathrm{S}} + (\eta^{\mathrm{S}} - \eta^{\mathrm{L}}) T_{\mathrm{amb}}} = \frac{c_i^{\mathrm{L}} - c_i^{\mathrm{S}}}{\eta^{\mathrm{LS}}(\epsilon T_{\mathrm{L}} - T_{\mathrm{S}})} \quad (2)$$

where we have assumed equal efficiency for the sky and load beam ($\eta^{\mathrm{L}} = \eta^{\mathrm{S}} =: \eta^{\mathrm{LS}}$). If we solve for the system temperature instead, we arrive at the familiar y-factor expression:

$$T_{\mathrm{sys},i} = \frac{\eta^{\mathrm{LS}}(\epsilon T_{\mathrm{L}} - T_{\mathrm{S}} y_i)}{y_i - 1} \quad (3)$$

with $y_i = c_i^{\mathrm{L}}/c_i^{\mathrm{S}}$ denoting the ratio of the load signal to the reference (cold sky) signal. For a system temperature of 3000 K, this ratio will be close to one. Because the Rayleigh Jeans temperature of the sky T_{S} at 500 GHz is only 0.003 K, and therefore negligible compared to a load temperature $T_{\mathrm{L}} \approx 300$ K, we find that we can equate to a very good approximation

$$T_{\mathrm{sys},i} = \frac{c_i^{\mathrm{S}}}{g_i}. \quad (4)$$

We get the power in terms of a Rayleigh-Jeans temperature for the antenna signal by taking the difference of main beam and sky signal and dividing by the gain for each channel i:

$$\begin{aligned} T_{\mathrm{A},i} &= \frac{1}{\eta^{\mathrm{A}}}\left(\frac{c_i^{\mathrm{A}} - c_i^{\mathrm{S}}}{g_i} + \eta^{\mathrm{S}} T_{\mathrm{S}} - (\eta^{\mathrm{S}} - \eta^{\mathrm{A}}) T_{\mathrm{amb}}\right) \\ &= \frac{1}{\eta^{\mathrm{A}}}\left(\frac{c_i^{\mathrm{A}} - c_i^{\mathrm{S}}}{c_i^{\mathrm{S}}} T_{\mathrm{sys},i} - T_{\mathrm{sp}}\right) \end{aligned} \quad (5)$$

where the spill-over contribution T_{sp} is mainly due to the difference in integrated gain of the main beam and the sky beam. Whereas η^{S} is expected to be very close to one, the value for η^{A} will be determined by the baffle which intercepts the main beam at the −17 dB level.

$$T_{\mathrm{sp}} = -\eta^{\mathrm{S}} T_{\mathrm{S}} + (\eta^{\mathrm{S}} - \eta^{\mathrm{A}}) T_{\mathrm{amb}} \approx (\eta^{\mathrm{S}} - \eta^{\mathrm{A}}) T_{\mathrm{amb}}. \quad (6)$$

The observed T_{sp} is around 10 K, corresponding to a value of $\eta^{\mathrm{A}} \approx 0.97$. This agrees very well with direct calculations based on the Odin quasi-optics design. Due to the pronounced gain variation during the course of an orbit (see Fig. 2) it is mandatory to use reference data c_i^{S} which are properly sampled onto the time of the signal measurement c_i^{A}, as described by e.g. Jarnot et al. (1996) for the UARS-MLS mission.

The processing usually works with data from one orbit at a time, and typically goes through the following sequence:

1. Extraction of spectral data from raw (level 0) science data (AC1, AC2 or AOS) files and sorting by phase: A, S and L.
2. Reconstruction of LO-frequency and side-band information from house-keeping data, including correction for temperature drifts.
3. Calculation of the telescope pointing from reconstructed attitude information. This step takes into account the best-known values for the misalignment of the telescope beam vs. the satellite control frame. These values are derived from mapping observations of Jupiter.
4. Discard spectra which are contaminated by the Earth's atmosphere, either in the main or sky beam.
5. Discard spectra which have uncertain attitude data. This uncertainty is stored with the attitude information and is available via the Kalman filtering process applied during the attitude reconstruction (Jacobsson et al. 2002).
6. Discard spectra which deviate strongly in mean intensity from the median value of spectra of the same phase. Such a deviation is typical for data taken during movements of the selection mirror, to which the spectrometers are not synchronised.
7. Convert all measurements of the hot load (phase L) into spectra of system temperature T_{sys}, using Eqs. (2) and (4).
8. Transform all signal spectra (phase S) into a antenna temperature scale according to Eq. (5).

5. Backends

A general description of correlators and acousto-optical spectrometers used in radio astronomy can be found in Rohlfs & Wilson (2000).

5.1. Auto-correlators

The two correlators on-board were built by the Swedish company Omnisys and are of hybrid type, using up to 8×112 MHz bands. Eight correlator chips provide 96 lags each. The centre IF of each sub-band is tuneable within a 500 MHz wide band in 1 MHz steps. The channel spacing ranges from 125 kHz in 1-band mode to 1 MHz in 8-band mode. The spectral resolution is twice the channel spacing due to the applied Hanning smoothing.

The 3-level correlation scheme used here is extensively discussed in the literature; Kulkarni & Heiles (1980) use a relation known as Price's theorem to arrive at the relation between the true correlation ρ and the measured, modified correlation coefficients r at lag τ. For the case $c_+ = -c_- = c$, where $c_\pm = \nu_\pm/\sigma$ are the threshold voltages divided by the standard deviation of the input noise, this relation can be expressed as:

$$r(\tau) = \frac{2}{\pi} \int_0^{\rho(\tau)} \frac{1}{\sqrt{1-x^2}} \exp\left(-\frac{c^2}{(1+x)}\right) \mathrm{d}x. \qquad (7)$$

The Odin correlators provide monitor channels to check the assumption of equal absolute values of the positive and negative threshold levels. From Kulkarni & Heiles (1980) we can then use the following approximation to invert the relation between ρ and r:

$$\rho(z) = Ar - \frac{(c^2-1)^2}{6}(Ar)^3 \quad \text{with} \quad A = \frac{\pi}{2}\exp\left(c^2\right) \qquad (8)$$

which is valid for $|\rho| < 0.86$. An approximation for large correlation coefficients $|\rho| > 0.86$ is not needed for the case of an autocorrelator. The measured coefficient in the first channel (r_0: "zero lag"), after extraction of the total power information, will be normalised to 1 and is not subject to the approximation. Typical values of correlator coefficients in the second channel, which can be used as an upper limit for all other lags are $|r_1| \sim 0.02$, which is well below the limit where approximation (8) gives excellent results.

5.2. Acousto-optical spectrometer

The AOS was built by a consortium of three French laboratories: LAS (Marseille), CESR (Toulouse) and the Radio Astronomy Department of the Paris-Meudon Observatory (Lecacheux et al. 1998).

The photo detector is a 1754 pixels, linear CCD with 1728 usable frequency channels with a spectral resolution of 1.0 MHz. The CCD video output is read out every 5 ms and digitised over 12 bits, in order to keep the noise statistics of the signal unmodified over a dynamical range greater than 10 dB. A pre-adder delivers the sum of four consecutive readouts to the on-board micro computer, which performs the final double buffer integration in synchronism with the radiometer and antenna pointing information. The on-board micro computer also performs instrument monitoring and manages communication with the Odin system unit.

In order to meet data volume constraints during the aeronomy programme, the AOS offers a number of read-out modes with either a reduced number of bytes per channel, or pre-averaged channel values over a selected part of the spectrum. The default mode used for astronomy observations delivers 1728 32-bit data over the full band. An internal frequency comb generator is switched on, once per orbit, for checking the AOS frequency calibration. The thermal environment of spectrometer is monitored via a number of temperature sensors, whose read-outs are stored within the house-keeping data and as part of the AOS science data.

6. Software design and processing pipeline

Raw science and house-keeping data are downloaded at Esrange and transferred to a data archive housed by the Parallel Data Centre (PDC) at the Royal Institute of Technology (KTH) in Stockholm. The PDC in turn notifies the Odin data centre at Onsala Space Observatory about the availability of new radiometer data files. These level 0 files are downloaded and merged with house-keeping data and reconstructed attitude information as outlined above. After proper intensity and frequency calibration they are again uploaded to PDC as level 1 data, where they become available to the scientific teams in the four participating countries. Astronomy level 1 data are stored using binary FITS tables. For the aeronomy data the HDF format was chosen instead.

All software development was carried out on a Linux based system using tools available as open source. A relational database is used for keeping track of data files and processing status. Algorithms for the data retrieval and calibration of the radiometer were developed in the form of a compiled subroutine library. Combined with modern, powerful scripting languages it is possible to quickly build batch procedures and test algorithms; but as well to construct larger programs including graphical user interfaces, database handling and scientific plotting routines.

Acknowledgements. Generous financial support from the Research Councils and Space Agencies in Canada, Finland, France and Sweden is gratefully acknowledged. M. Olberg also acknowledges the work of the many developers of free software, which has contributed much to this project.

References

Frisk, U., Hagström, M., Ala-Laurinaho, J., et al. 2003, A&A, 402, L27
Hjalmarson, Å., Frisk, U., Olberg, M., et al. 2003, A&A, 402, L39
Jarnot, R. F., Cofield, R. E., Waters, J. W., Flower, D. A., & Peckham, G. E. 1996, J. Geophys. Res., 101, 9957
Jacobsson, B., Nylund, M., Olsson, T., Vandermarcq, O., & Vinterhav, E. 2002, IAC-02-A-4.01, World Space Congress 2002 (Houston)
Kulkarni, R. S., & Heiles, C. 1980, AJ, 85, 1413
Lecacheux, A., Rosolen, C., Michet, D., & Clerc, V. 1998, in Advanced Technology MMW, Radio and TeraHertz telescopes, ed. T. G. Phillips, Proc. SPIE, 3357, 519
Murtagh, D., Frisk, U., Merino, F., et al. 2002, Can. J. Phys., 80, 309
Pagani, L., Olofsson, A. O. H., Bergman, P., et al. 2003, A&A, 402, L77
Rohlfs, K., & Wilson, T. L. 2000, Tools of Radio Astronomy, 3rd ed. (Berlin: Springer Verlag)